

Optimization of the squeezing factor by temperature-dependent phase shift compensation in a doubly resonant optical parametric oscillator

Cite as: Appl. Phys. Lett. **115**, 171103 (2019); doi: [10.1063/1.5115795](https://doi.org/10.1063/1.5115795)

Submitted: 20 June 2019 · Accepted: 10 October 2019 ·

Published Online: 21 October 2019



View Online



Export Citation



CrossMark

Wenhui Zhang,¹ Jinrong Wang,¹ Yaohui Zheng,^{1,2,a)}  Yajun Wang,^{1,2,b)}  and Kunchi Peng^{1,2}

AFFILIATIONS

¹State Key Laboratory of Quantum Optics and Quantum Optics Devices, Institute of Opto-Electronics, Shanxi University, Taiyuan 030006, China

²Collaborative Innovation Center of Extreme Optics, Shanxi University, Taiyuan, Shanxi 030006, China

^{a)}yhzheng@sxu.edu.cn

^{b)}Author to whom correspondence should be addressed: wangyajun_166@163.com

ABSTRACT

We report on a compensation characteristic of the phase shifts, originating from the cavity detuning and phase mismatching, in the process of squeezed state generation. In the experiment, the maximum level of squeezing was not generated under coresonance in a doubly resonant optical parametric oscillator (OPO), which was theoretically explained based on the motion equation of the OPO. Furthermore, the power dependence of the squeezing and antisqueezing was also measured at the coresonance and the optimum noise reduction status. The results revalidated the compensation mechanism. Finally, the amplitude quadrature (or vacuum) noise reduction was raised to 11.7 dB (or 12.3 dB) at 8 MHz by finely tuning the crystal temperature away from coresonance.

Published under license by AIP Publishing. <https://doi.org/10.1063/1.5115795>

Squeezed states can be prepared during the second or third order nonlinear interaction in a nonlinear medium,¹⁻³ in which the quantum noise of the quadrature components of vacuum or coherent light is improved beyond the quantum noise limit (QNL). Pervasive significant applications were carried out with squeezing technology, for example, continuous wave cluster state generation for quantum computing and networks,⁴⁻⁹ small spatial displacement measurements,^{10,11} gravitational wave detection,^{12,13} and quantum radar.^{14,15} All of these applications address the requirement of high squeezing strength with as little laser power consumption as possible,¹⁶⁻¹⁸ and every little bit of additional quantum noise reduction could be critical for quantum sensing and computing applications. Squeezing strength is mainly limited by the optical losses (mixing vacuum noise into the squeezed field) and phase fluctuations (projecting the noise of antisqueezed quadrature onto the squeezed one) in the processes for squeezing production, transfer, and detection.^{19,20}

The optical parametric oscillator (OPO) is a common approach for generating a strong squeezing,^{16,17} which contains a resonator to enhance the nonlinear interaction. Squeezing occurs on a certain quadrature component, at the expense of increasing noise power in its orthogonal one. The squeezed quadrature is mainly dependent on the

relative phase θ_B between the signal and pump beams. For $\theta_B = 0$, the phase quadrature is squeezed. For $\theta_B = \pi$, the amplitude quadrature noise is reduced below the QNL. However, the squeezing angle may be shifted from the amplitude or phase component owing to cavity detuning or phase mismatching.²⁰⁻²² A singly resonant OPO is easy to meet the resonance for the signal beam at the phase matching temperature, but it consumes more pump power than the doubly resonant one.²³

The dual resonator is benefit for lowering the threshold power of the OPO, but it is a challenge to simultaneously achieve double resonance as well as the optimum phase matching conditions. Usually, the double resonance is maintained by locking the cavity to the pump beam and precisely controlling the nonlinear crystal temperature and ensuring the temperature close to the phase matching one as much as possible. In Ref. 18, double resonance and close to optimum quasi-phase matching were simultaneously achieved by coarse trial and error adjustment of the Gouy phase via the cavity length, together with fine tuning of the crystal temperature. The authors claimed that compensation between differential phase shifts in mirror coatings of the high reflectors of the OPO and the Gouy phase during the nonlinear interaction was possible, either by adjusting the Gouy phase via cavity

length or by designing proper dielectric mirror coatings with the theoretical models in Ref. 24. After these optimizations, the total phase made sure that the nonlinear interaction reaches a maximum value. In practice, the doubly resonant temperature is inevitable to have a small difference with the phase matching one. Therefore, we only assure that one status meets the optimum value for each measurement and slightly sacrifices the other. Nevertheless, small variation in the cavity length (breaking the resonant condition) or phase matching will draw into a phase shift to rotate the squeezing angle,^{20–22} which makes the measured quadrature component deviate from the maximum squeezing one. However, the phase fluctuation dependence of the squeezing becomes acute with the increase in the squeezing strength, which should be thoroughly quantified and reduced as far as possible.^{23,25}

In this Letter, in terms of the physical condition of coresonance, a doubly resonant cavity was designed by considering both the crystal length and the cavity air gap distance. Meanwhile, we demonstrated a compensation characteristic of the phase shifts, originating from the cavity detuning and the phase mismatching, during the squeezed state generation. Based on the motion equation of the OPO, the compensation mechanism was theoretically explained. By measuring repeatedly the power dependence of the squeezing and the antisqueezing under the coresonance and the optimal noise reduction status, we confirmed the analysis results again. Finally, at the coresonant temperature, an optimal quantum amplitude (vacuum) noise reduction of 11.3 dB (12 dB) at 8 MHz was obtained. The squeezed level was raised to 11.7 dB (12.3 dB) at 8 MHz by carefully optimizing the crystal temperature away from coresonance.

The experimental scheme is shown in Fig. 1. The fiber laser, with 1 W output power at 1550 nm, is divided into two beams. One is injected into a mode cleaner (MC1) to improve the fundamental spatial-temporal mode and reduce the intensity noise at the radio frequency (RF) region. Its output is prepared for the local oscillator (LO) of the balanced homodyne detection (BHD), as well as the auxiliary (or seed) beam of aligning the OPO. The remaining part (210 mW) is injected into the second harmonic generator (SHG) to produce an upconversion lasing of 100 mW as a pump source of the OPO. The OPO is constituted by a concave mirror and a periodically poled titanyl phosphate crystal (PPKTP, Raicoll Crystals Ltd.). The PPKTP is 10 mm long (L_c) with a curvature radius of 12 mm and high reflectivity

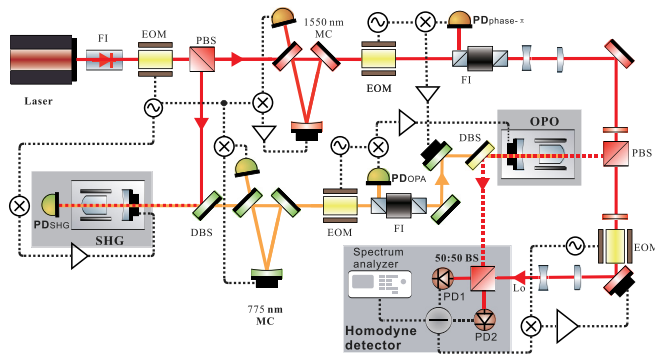


FIG. 1. The schematic of the squeezed state generator. FI, Faraday isolator; EOM, electro-optical modulator; PBS, polarization beam splitter; SHG, second harmonic generator; MC, mode cleaner; OPO, optical parametric oscillator; DBS, dichroic beam splitter; PD, photodetector; and BHD, balanced homodyne detection.

(HR) both at 1550 nm and 775 nm, and the plane surface is antireflection (AR) coated. The concave mirror acts as an output coupler with a curvature radius of 25 mm, and its reflectivities for 1550 nm and 775 nm are 84.3% and 97.8%, respectively. The fineness (linewidth) of the fundamental and harmonic waves is 34.7 (110.4 MHz) and 200 (19 MHz), respectively. The escape efficiency of the OPO is about $98\% \pm 0.47\%$, corresponding to a threshold pump power of 16.7 mW. The visibility of the local and signal beam in BHD is better than 99.5%, and the two photodiodes have a quantum efficiency of more than 99% (Laser Components).

PPKTP has a wide temperature full width at half maximum (FWHM) of about 14°C with a poled period of $24.7\ \mu\text{m}$ for the wavelength conversion of 1550 nm and 775 nm, which imposes less strict conditions on the temperature stabilization. Therefore, it is easier to achieve the doubly resonant status. The dispersion compensation was achieved by finely tuning the crystal temperature with a high precision (0.001°C) temperature controller (Thorlabs, TED4015). The OPO cavity length was locked to the pump beam by the Pound-Drever-Hall (PDH) technique. The temperature dependence of the conversion efficiency was measured by scanning the temperature of the crystal with a fundamental wave injected, and the measurement results were fitted with a sinc function, shown in the red dots and a black line of Fig. 2(b). The slope of the blue line in Fig. 2(b) represents the coresonant status for different air gaps when heating the crystal at different temperatures. The phase matching temperature T_p equals 43.77°C .

The coresonant status is analyzed by simultaneously considering the phase matching temperature and the cavity length L . The physical condition for coresonance is that the round trip phase delay for the circular beam in the resonator must be an integer of 2π , i.e., $\theta_{\omega(2\omega)} = k_{\omega(2\omega)} \cdot 2L + \theta_{0\omega(02\omega)} = 2\pi h_{1(2)}$ [$h_{1(2)}$ is an integer, $k_{\omega(2\omega)}$ is the wavenumber of the fundamental beam (pump beam), and $\theta_{0\omega(02\omega)}$ is an initial phase of the fundamental beam (pump beam)].²⁶ The cavity length L is expressed as $n_{\omega,2\omega} \cdot L_c + L_{ag} \cdot n_{\omega}$ and $n_{2\omega}$ are the refractive index of the fundamental and harmonic waves.²⁷ Then, the crystal

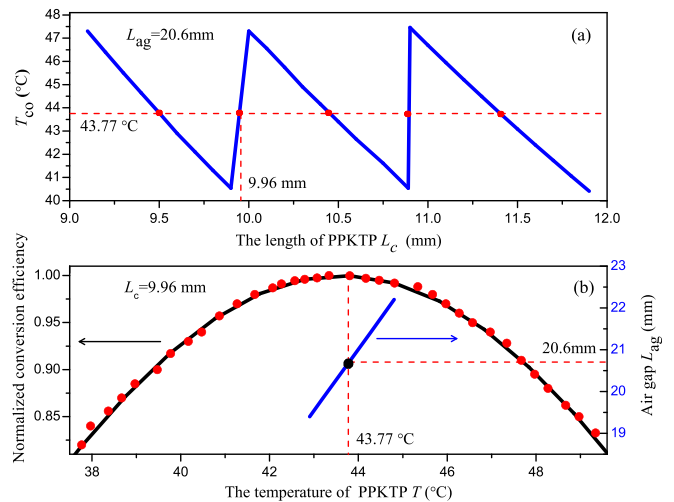


FIG. 2. The theoretical results of coresonant temperatures in the temperature bandwidth of the PPKTP crystal for different (a) crystal lengths L_c and (b) air gap lengths L_{ag} of the cavity.

length and the air gap distance were theoretically designed by simultaneously considering the phase matching temperature, which are shown in Fig. 2. First, for a certain air gap, e.g., $L_{ap} = 20.6$ mm, the coresonant condition was calculated as a function of L_c and shown as the solid line in Fig. 2(a), which exhibits a periodical variation with L_c . At the optimal phase matching temperature, the OPO can operate on double resonance for some discrete L_c [red dot in Fig. 2(a)]. Subsequently, for a given crystal length $L_c = 9.96$ mm, then the coresonant status can be figured up near the optimal phase matching temperature by continuously changing L_{ap} [shown as the blue linear line in Fig. 2(b)]. Only at the black cross point of the blue line in Fig. 2(b), coresonance will overlap with the perfect phase matching condition. Finally, we can ensure that the OPO operates on coresonance at $T_p = 43.77$ °C with $L_c = 9.96$ mm and $L_{ap} = 20.6$ mm.

In the actual situation, limited by mismachining tolerance, operational error of the cavity length and crystal parameters, and differential phase shifts (difficult to control and evaluate),²⁴ the experimental results for coresonant status might inevitably deviate from the ideal one. Therefore, when the OPO operates on coresonance, the nonlinear crystal temperature might separate from T_p and introduce a phase mismatching factor Δk . As a result, the nonlinear coupling parameter should be modified to $\varepsilon = \varepsilon_0 e^{-\frac{\Delta k L_c}{2}} \sin c\left(\frac{\Delta k L_c}{2}\right)$, where ε_0 is the nonlinear coupling parameter for optimal phase matching temperature. ε decays exponentially with the phase mismatching factor Δk , which has an adverse impact on the squeezing quadrature by introducing a phase shift $\Delta\theta_k = \frac{\Delta k L_c}{2} = v(T - T_p) = v\Delta T$.^{20,21,28} ΔT is a temperature offset away from T_p . v is a constant, corresponding to the temperature coefficient of the optical path variation.²⁰ In order to realize the coresonant condition at T_p , a wedge component was usually adopted to compensate the dispersion induced by the differential path length for the two resonant modes,^{29,30} but it is not feasible for a half-monolithic OPO with one crystal surface to be used as a spherical cavity mirror.

Additionally, a temperature deviation δT of the PPKTP will break the coresonant status and introduce a cavity detuning for the seed beam, $\Delta_L = \omega\delta L/L$ (ω is the laser frequency). The effect of the detuning is equivalent to a phase shift $\Delta\theta_L$ of the seed beam, which rotates the squeezing angle and degrades the measured squeezing. In this case, the total phase shift $\Delta\theta_B$ is the combination of the effect from cavity detuning and phase mismatching. Subsequently, we expect to verify and demonstrate a mutual compensation characteristic of the two phase shifts.

The composite effect on the squeezing for the two phase shifts can be quantified by the motion equation of the OPO in matrix form,^{21,22,28}

$$\dot{\chi}_c = \gamma_a^{\text{tot}} \mathbf{M}_c \chi_c + \mathbf{M}_{in} \chi_{in} + \mathbf{M}_{out} \chi_{out} + \mathbf{M}_l \chi_l, \quad (1)$$

where the matrices $\mathbf{M}_i = \sqrt{2}\gamma_i \mathbf{I}$ ($i = \text{in, out, and l}$) are the effect of the input mirror coupling rate γ_{in} , output mirror coupling rate γ_{out} , and round trip loss coupling rate γ_l on the squeezing production, and \mathbf{I} is a 2×2 identity matrix. The matrix

$$\mathbf{M}_c = \begin{pmatrix} -1 + i \frac{\Delta_L}{\gamma_a^{\text{tot}}} & x \sin c(\Delta\theta_k) e^{i(\theta_B - \Delta\theta_k)} \\ x \sin c(\Delta\theta_k) e^{-i(\theta_B - \Delta\theta_k)} & -1 - i \frac{\Delta_L}{\gamma_a^{\text{tot}}} \end{pmatrix} \text{ includes}$$

three quantities (Δ_L , x , and $\Delta\theta_k$) in connection with the squeezing

strength. x is the normalized nonlinear interaction strength, $x = |\varepsilon| |\beta| / \gamma_a^{\text{tot}}$ ($\beta = |\beta| e^{i\theta_B}$), where β is the amplitude of the pump field. The parameter γ_a^{tot} is the total resonator decay rate for the fundamental field. χ_c , χ_{in} , χ_{out} , and χ_l are the column matrices for the annihilation and creation operators. The matrix elements in \mathbf{M}_c can be divided into two parts. The first two diagonal elements are the detuning part, which introduce a phase shift to the signal beam, and the other two diagonal elements are the phase mismatching part, which shift the phase of the pump beam and reduce the nonlinear interaction strength. Consequently, they codetermine the noise reduction of the OPO output by rotating the squeezing angle. With Eq. (1), the phase shifts originating from the two effects can be calculated, respectively. The analysis results showed that the phase shifts $\Delta\theta_L$ and $\Delta\theta_k$ can be operated to have an opposite sign with the change of crystal temperature.²⁰ Originally, the crystal temperature was controlled to meet the coresonant status but might not equal the optimal phase matching temperature T_p . If we optimize the squeezing strength by tuning the temperature toward to T_p , the phase shift induced by the cavity detuning will compensate that induced by the phase mismatching to some extent. Thus, the squeezing strength may be optimized to a higher level by only tuning the nonlinear crystal temperature.

Experimentally, the OPO length was designed for a certain L_c (9.96 mm) and L_{ap} (20.6 mm) on the basis of the theoretical result. First, the output mirror of the OPO was fixed to the main architecture of the cavity, and the PPKTP was carefully placed into the copper of the crystal to achieve the designed cavity length for coresonant status. Subsequently, the coresonant status was realized, by finely tuning the temperature of the PPKTP after locking the OPO to resonate with the pump field and monitoring the maximum classical gain of the signal beam with a seed beam being injected. The seed beam also acted as a sensor of the relative phase during the squeezed state generation. Comparing the coresonant temperature with T_p , if they have a large difference, we should change the distance of L_{ap} by moving the PPKTP to a new position along the optical axis of the OPO. Finally, we iterated several times the adjustment of the air gap around 20.6 mm and then the dual resonance could be operated near phase matching temperature. After the optimization of the coresonant status, the relative phase between the pump beam and the signal beam was locked to π and the relative phase of the local beam and the signal beam in the BHD was locked to 0 (or $\pi/2$). The amplitude quadrature squeezed state was measured with a spectrum analyzer (SA) at the analysis frequency of 8 MHz, with a resolution bandwidth (RBW) of 300 kHz and a video bandwidth (VBW) of 200 Hz. The maximum noise reduction of 11.3 dB was obtained at the pump power of 13.5 ± 0.5 mW. By tuning the crystal temperature, the temperature dependence of the squeezing (antisqueezing) was experimentally observed, and shown as the dot (triangular) symbols in Fig. 3. The solid lines in Fig. 3 were the fitting results according to the measured values and model in Eq. (1). When the crystal temperature detuned 0.1 ± 0.01 °C from coresonance, the maximum noise reduction of 11.7 dB was directly observed.

The experimental results can be explained by the former analysis. If not considering the phase shift originating from nonlinear coupling parameter ε , the temperature deviation from coresonance will introduce a cavity detuning of the fundamental wave. It brings an additional phase shift into the fundamental field and finally degrades the squeezing strength, which conflicts with the experimental results in Fig. 3. When considering the influence of the parameter ε , there was

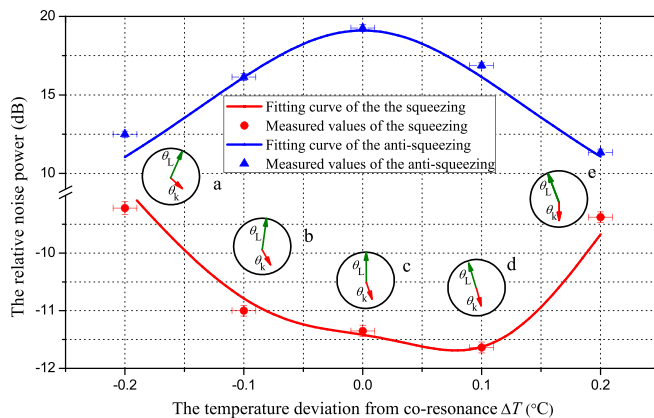


FIG. 3. The quadrature noises as a function of temperature deviation from the co-resonance of the OPO. The illustrations (a)–(e) present the relative phase evolutionary process due to the phase mismatching θ_k and cavity detuning θ_L with the temperature change around the co-resonance.

another phase shift, except for the cavity detuning. In the experiment, the crystal temperature at co-resonant status was not T_p , and hence, it is involved in a phase shift to decrease the squeezing. Gradually changing the temperature around co-resonance, the original phase shift might be partially or completely compensated by the cavity detuning (point d in Fig. 3). Further tuning the temperature away from the compensated point, the decreased ε due to cavity detuning reduced the squeezing strength quickly (point e in Fig. 3). Tuning the temperature to the opposite direction, the complex phase shift increased the phase difference, which further lowered the squeezing strength. The evolution diagram of the temperature-dependent phase differences is presented by the clock-like circular motion in Fig. 3. The antisqueezing was immune to the phase difference, which followed the general evolution rule with the crystal temperature. The experimental results of the squeezing and anti-squeezing strength were perfectly in agreement with the theoretical analysis. The results provide guidance to optimize the squeezing strength as far as possible. Although resonant status can be conveniently transformed by changing the cavity length and the crystal temperature within the TFWHM on a large scale, our method was yet limited by the linewidth of the OPO resonator and only suited to a small temperature range due to the 110 MHz linewidth for the squeezing beam. Therefore, a wider bandwidth OPO is more benefit to implement the phase compensation by tuning the crystal temperature. Our method provides an effective approach for improving the squeezing strength in the doubly resonant OPO under the nonperfect phase matching condition.

Figure 4 shows the dependence of the squeezing and antisqueezing on the pump power. A squeezed vacuum state, with the maximum noise reduction of 12.3 dB (12.5 dB by considering the electronic noise) and a pump power of 13.5 ± 0.5 mW, was experimentally measured by optimizing the crystal temperature near the co-resonant status. The solid rhombuses and triangle dots were the measured squeezing and antisqueezing and were fitted on the basis of the theoretical model of Eq. (1) (the solid line). There were a total optical loss of $5\% \pm 0.15\%$ and a phase fluctuation of 1.4 ± 0.26 mrad. We repeated the measurement at the co-resonant point. The hollow rhombuses and triangle dots were the measured squeezing and antisqueezing corresponding to a noise reduction of 12 dB; the result was fitted

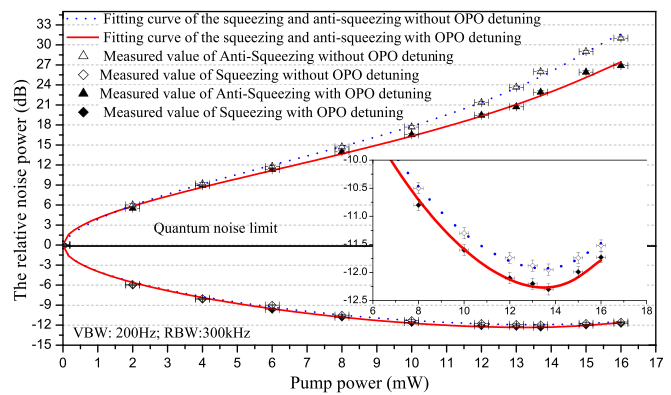


FIG. 4. Pump power dependence squeezing and antisqueezing quadrature noise with experimental and theoretical results.

with a total optical loss of $5\% \pm 0.15\%$ and a phase fluctuation of 4 ± 0.32 mrad. It further confirmed that the analysis above was valid (dotted line). The difference of the squeezing strength between the bright squeezed state and squeezed vacuum state was attributed to the noise coupling of the seed beam to the pump beam.^{31,32}

In conclusion, we demonstrated a design of a doubly resonant OPO, by considering both the crystal length and the air gap distance, and proposed a phase shift compensation mechanism, originating from the imperfect temperature overlap between the co-resonance and phase matching. Based on the motion equation of the OPO, we theoretically explained this mechanism in the quadrature squeezing production process.

For a doubly resonant OPO, the co-resonant temperature was practically impossible to completely overlap with T_p , which would bring into a phase shift due to phase mismatching and reduce the squeezing strength. In the experiment, we gradually adjusted the crystal temperature detuning from doubly resonant status, whereafter a further quadrature noise reduction of 11.7 dB at 8 MHz was directly measured, which confirmed a phase shift compensation method based on the theoretical model. We repeatedly measured the power dependence of the squeezing and antisqueezing at the co-resonance and the optimum noise reduction status. The fitting results for the phase fluctuation were in good agreement with the experimental and theoretical results of the compensation mechanism. The results provide guidance to optimize the squeezing strength as much as possible.

This work was supported by the National Natural Science Foundation of China (NSFC) (Nos. 11654002, 61575114, 11874250, 11804207, and 61574087); National Key Research and Development Program of China (No. 2016YFA0301401); Program for Sanjin Scholar of Shanxi Province; Program for Outstanding Innovative Teams of Higher Learning Institutions of Shanxi; and Fund for Shanxi “1331 Project” Key Subjects Construction.

REFERENCES

- ¹L. A. Wu, H. J. Kimble, J. L. Hall, and H. Wu, *Phys. Rev. Lett.* **57**, 2520 (1986).
- ²A. Thüring and R. Schnabel, *Phys. Rev. A* **84**, 033839 (2011).
- ³M. R. Huo, J. L. Qin, Y. R. Sun, J. L. Cheng, Z. H. Yan, and X. J. Jia, *Acta Sin. Quantum Opt.* **24**, 134–140 (2018).

- ⁴X. L. Su, C. X. Tian, X. W. Deng, Q. Li, C. D. Xie, and K. C. Peng, *Phys. Rev. Lett.* **117**, 240503 (2016).
- ⁵A. Ourjountsev, R. Tualle-Brouri, J. Laurat, and P. Grangier, *Science* **312**, 83–86 (2006).
- ⁶N. C. Menicucci, P. V. Loock, M. Gu, C. Weedbrook, T. C. Ralph, and M. A. Nielsen, *Phys. Rev. Lett.* **97**, 110501 (2006).
- ⁷J. Yoshikawa, S. Yokoyama, T. Kaji, C. Sornphiphatphong, Y. Shiozawa, K. Makino, and A. Furusawa, *APL Photon.* **1**, 060801 (2016).
- ⁸M. Chen, N. C. Menicucci, and O. Pfister, *Phys. Rev. Lett.* **112**, 120505 (2014).
- ⁹M. Huo, J. Qin, J. Cheng, Z. Yan, Z. Qin, X. Su, and K. Peng, *Sci. Adv.* **4**, eaas9401 (2018).
- ¹⁰R. C. Pooser and B. Lawrie, *Optica* **2**, 393–399 (2015).
- ¹¹N. Treps, N. Grosse, W. P. Bowen, C. Fabre, H. A. Bachor, and P. K. Lam, *Science* **301**, 940–943 (2003).
- ¹²T. Eberle, S. Steinlechner, J. Bauchrowitz, V. Händchen, H. Vahlbruch, M. Mehmet, H. Müller-Ebhardt, and R. Schnabel, *Phys. Rev. Lett.* **104**, 251102 (2010).
- ¹³E. Oelker, G. Mansell, M. Tse, J. Miller, F. Matichard, L. Barsotti, P. Fritschel, D. E. McClelland, M. Evans, and N. Mavalvala, *Optica* **3**, 682–685 (2016).
- ¹⁴Z. Dutton, J. H. Shapiro, and S. Guha, *J. Opt. Soc. Am. B* **27**, A63–A72 (2010).
- ¹⁵S. Lloyd, *Science* **321**, 1463–1465 (2008).
- ¹⁶H. Vahlbruch, M. Mehmet, K. Danzmann, and R. Schnabel, *Phys. Rev. Lett.* **117**, 110801 (2016).
- ¹⁷S. Shi, Y. Wang, W. Yang, Y. Zheng, and K. Peng, *Opt. Lett.* **43**, 5411–5414 (2018).
- ¹⁸A. Schänbeck, F. Thies, and R. Schnabel, *Opt. Lett.* **43**, 110–113 (2018).
- ¹⁹P. K. Lam, T. C. Ralph, B. C. Buchler, D. E. McClelland, H. Bachor, and J. R. Gao, *J. Opt. B* **1**, 469 (1999).
- ²⁰S. Dwyer, L. Barsotti, S. S. Y. Chua, M. Evans, M. Factourovich, D. Gustafson, T. Isogai, K. Kawabe, A. Khalaidovski, P. K. Lam, M. Landry, N. Mavalvala, D. E. McClelland, G. D. Meadors, C. M. Mow-Lowry, R. Schnabel, R. M. S. Schofield, N. Smith-Lefebvre, M. Stefszky, C. Vorvick, and D. Sigg, *Opt. Express* **21**, 19047–19060 (2013).
- ²¹K. McKenzie, M. B. Gray, P. K. Lam, and D. E. McClelland, *Opt. Express* **14**, 11256–11264 (2006).
- ²²C. Fabre, E. Giacobino, A. Heidmann, L. Lugiato, S. Reynaud, M. Vadamchino, and K. Wang, *Quantum Opt.* **2**, 159 (1990).
- ²³W. H. Yang, S. P. Shi, Y. J. Wang, W. G. Ma, Y. H. Zheng, and K. C. Peng, *Opt. Lett.* **42**, 4553–4556 (2017).
- ²⁴N. Lastzka and R. Schnabel, *Opt. Express* **15**, 7211–7217 (2007).
- ²⁵D. B. Horoshko and M. I. Kolobov, *Phys. Rev. A* **88**, 033806 (2013).
- ²⁶T. Juwiler, A. Arie, A. Skliar, and G. Rosenman, *Opt. Lett.* **24**, 1236–1238 (1999).
- ²⁷S. Emanuelli and A. Arie, *Appl. Opt.* **42**, 6661–6665 (2003).
- ²⁸K. Goda, K. McKenzie, E. E. Mikhailov, P. K. Lam, D. E. McClelland, and N. Mavalvala, *Phys. Rev. A* **72**, 043819 (2005).
- ²⁹S. S. Y. Chua, M. S. Stefszky, C. M. Mow-Lowry, B. C. Buchler, S. Dwyer, D. A. Shaddock, P. K. Lam, and D. E. McClelland, *Opt. Lett.* **36**, 4680–4682 (2011).
- ³⁰K. C. Peng, Q. Pan, H. Wang, Y. Zhang, H. Su, and C. D. Xie, *Appl. Phys. B* **66**, 755–758 (1998).
- ³¹K. McKenzie, N. Grosse, W. P. Bowen, S. E. Whitcomb, M. B. Gray, D. E. McClelland, and P. K. Lam, *Phys. Rev. Lett.* **93**, 161105 (2004).
- ³²X. C. Sun, Y. J. Wang, L. Tian, S. P. Shi, Y. H. Zheng, and K. C. Peng, *Opt. Lett.* **44**, 1789–1792 (2019).